

## Dynamic adsorption characteristics of thin layered activated charcoal materials used in chemical protective overgarments

Radovan M Karkalic<sup>1,a</sup>, Negovan D Ivankovic<sup>1</sup>, Dalibor B Jovanovic<sup>2</sup>, Smiljana M Markovic<sup>3</sup>, Dejan R Indjic<sup>1</sup>, Marija D Micovic<sup>4</sup> & Branko V Kovacevic<sup>5</sup>

<sup>1</sup>University of Defence, Military Academy, Belgrade, Serbia

<sup>2</sup>Technical Test Center, Serbian Armed Forces Generalstaff, Serbia

<sup>3</sup>Faculty of Technological Sciences, University of Pristina, Kosovska Mitrovica, Serbia

<sup>4</sup>The Academy of Criminology and Police Studies, Belgrade, Serbia

<sup>5</sup>Chemical Biological Radiological Nuclear Training Center, Serbian Armed Forces Generalstaff, Serbia

*Received 5 January 2015; revised received and accepted 5 May 2015*

The efficiency of a thin layered activated charcoal material used in chemical protective overgarments has been evaluated. The study has been conducted with the aim to obtain protective materials with best characteristics considering resistance to benzene effect under dynamic conditions and to create a new filtration protection device. In order to evaluate dynamic adsorption characteristics of thin layered sorption materials, sophisticated dynamic gas chromatography method is used. The curves of benzene penetration are determined for sandwich materials, and sorption layers used in filtrating protective clothing shows that thin layered carbon sorption materials (type M00) have good protective properties as compared to other similar materials. The findings will help to create conditions for developing a functional model for producing a new protective overgarment in the near future.

**Keywords:** Activated charcoal, Gas chromatography, High toxic contamination, Protective clothing

### 1 Introduction

Chemical protective overgarments (CPO) represent a modern body protection covering, as accepted by many developed countries. It's a new concept of textile materials where the thin layered sorption materials are kept as sandwich materials, using outerlayer (cotton+polyester) and innerlayer (activated charcoal or activated charcoal+polyurethane foam). Filtrating protective materials are permeable to water and water vapor, which makes them physiologically much more acceptable than the isolating materials.

These overgarments allow their users to stay for a much longer duration on contaminated ground, thus enabling them to perform more complex tasks<sup>1-3</sup>. These protective suits can be worn over undergarments or, in colder weather over clothing or regular military uniforms. They can be made as one piece or two piece suits. CPOs need to have good protective, physiological, mechanical and other practical properties which make them much more demanding. Considering the current technological

advances in the area, all CPOs should be made out of two thin layers of permeable materials (outer and inner layer)<sup>4-6</sup>. Given that the outer layer is usually made out of cotton and polyester combination, there is a possibility of dyeing the fabric in multiple color masking patterns. In accordance with that there are different garment masking patterns depending on the masking needs of users in different parts of the world.

In this type of garment, hazardous gases are kept aside by means of adsorption conducted by filter fabrics containing activated carbon. Textile filter fabrics of nonwoven or polyurethane foam are loaded with activated carbon powder. Other technologies use a carbonized and activated woven or knit fabric fixed onto a textile carrier.

The specific material, covered with active charcoal has a high flexibility, high air permeability and low thickness, which together provide very high wearer comfort<sup>7-9</sup>. The two layers and the air gap provide comfort and efficient body heat control under all climatic conditions. The suit employs spherical carbon technology to provide effective body protection from well-known chemical/biological warfare agents while offering the best possible flow

<sup>a</sup>Corresponding author.  
E-mail: rkarkalic@yahoo.com

conditions for body heat dissipation, so that the suit stays as cool as possible. The activated carbon provides additional protection against chemical warfare agents in liquid, vapor and aerosol forms (Fig. 1).

The present study was therefore aimed at evaluating the efficiency of a contemporary thin layered activated charcoal materials used in chemical protective overgarments. The study was conducted with the aim to obtain protective materials with best characteristics considering resistance to benzene effect under dynamic conditions and to create a new filtration protection device.

## 2 Materials and Methods

In order to evaluate dynamic adsorption characteristics of thin layered sorption materials, a sophisticated dynamic gas chromatography method (DGCM) was used, considering benzene as a reference adsorbent. Benzene is an organic chemical compound - a highly toxic chemical. Benzene, by the virtues of its characteristics, can be taken as a representative of a large group of highly toxic chemicals. The effects of benzene vapors on CPO samples depend on adsorption dynamics which represents a basis for the purification of contaminated air with filtrating materials.

The dynamic gas chromatography method is a unique, sophisticated instrumental method for testing

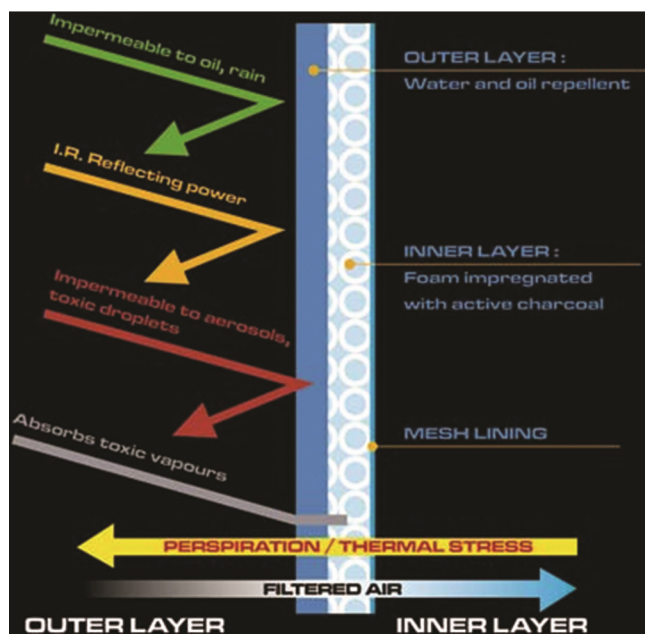


Fig. 1 — Material with activated carbon - outer and inner layer (<http://www.PaulBoye/PaulBoye-Presentation.htm>)

of filtrating protective materials in the laboratory conditions. The existence of the asymptotic concentration profile in the sorption layer makes it possible to determine adsorption isotherm up to the entry concentration of the adsorbent from the breakthrough curve using the dynamic method. Experiments conducted in dynamic conditions and analytical method have three basic advantages over static method of determining adsorption capacities at low adsorbent, as shown below:

- (i) As the dynamic method uses more sensitive detectors, it is more suitable for work with lower concentrations than the static method.
- (ii) The dynamic method is specific because gas chromatograph column separates adsorbent which is used for determining capacity from the other substances (impurities) that are often present.
- (iii) The dynamic method simulates conditions close to the ones we meet in a practical application of the adsorbent.

### 2.1 Materials

Chemical protective overgarments produced by Traylor Corporation in Serbia, and Helsa Werke, Kärcher and Blücher in Germany were used. These protective garments are comparable as they are produced with two layers (sandwich materials). The outerlayer is made from cotton (67 %) and polyester (33 %), and the innerlayer from activated carbon spheres or combination of activated carbon and polyurethane foam. Following materials were used in this study:

- (i) Protective garments (sandwich materials) produced in Serbia, such as M1, M2, M2PUR and M00
- (ii) Other protective garments sandwich materials such as:
  - material with a carrier on the basis of polyurethane foam (Helsasafe 2084), developed by Helsa Werke, Germany (named HSF<sub>pur</sub> 2084),
  - material with a carrier on the basis of filter cloth type Saratoga<sup>TM</sup> (Safeguard 3002), developed by Kärcher, Germany (named SFG<sub>stg</sub> 3002), and
  - material with a carrier on the basis of filter cloth (type Saratoga<sup>TM</sup>), developed by Blücher, Germany (named BCH<sub>stg</sub>).

The samples of circular shape sandwich materials (area  $A_u = 10 \text{ cm}^2$ ) were used. Similarly, the samples of sorption layers of these materials were used without the first layer (outer camouflage layer).

Before the examination, all the samples were dried in an electric dryer at 105 °C and then preserved in an excicator above potassium chloride.

## 2.2 Equipments

The apparatus needed to determine gas/vapor breakthrough curves are given below<sup>10</sup>:

- Gas chromatograph (GC) (Hewlett Packard, model HP 5890A), with flame ionizing detector (FID), steel neutral column (SE 30) and automated pneumatic tap with ten openings and two loops (each 0.5 cm<sup>3</sup> in volume), used for automatic sampling of appropriate gas mixture for analysis; computed with interface, printer, plotter and appropriate data analysis software,
- DYNA-calibrator and diffusion pipe for examining substance in liquid form,
- Peristaltic pump for analyzed gas mixture to flow through the chromatograph,
- Flow meter up to 300 cm<sup>3</sup>/min,
- Flow regulation needle tap, and
- Steel bottle with nitrogen, air and hydrogen for supplying them to flame-ionizing detector, and steel bottle with nitrogen for maintaining pressure on pneumatic electromagnetic tap.

As an adsorbant, benzene (C<sub>6</sub>H<sub>6</sub>) of p.a. purity [physical constants: molecular mass (*M*) 78.11 g/mol, density ( $\rho_{296K}$ ) 0.876 g/cm<sup>3</sup>, boiling point (*T<sub>b</sub>*) 80.1 °C, saturated vapor concentration at 23 °C (*C<sub>s</sub>*) 367 g/m<sup>3</sup>, vaporization latent heat (heat of condensation) ( $\lambda_{23\text{ }^\circ\text{C}}$ ) 33.614 kJ/mol and liquid refraction index at wavelength of sodium's D line [ $(\eta_{D, 25\text{ }^\circ\text{C}}) = 1.49576$ ] was used.

Figure 2 shows the schematic diagram of the apparatus for determining the benzene breakthrough curve, according to the modified Yoon-Nelson model (MYNM)<sup>11</sup>.

The steps of GC/FID system calibration process using benzene are:

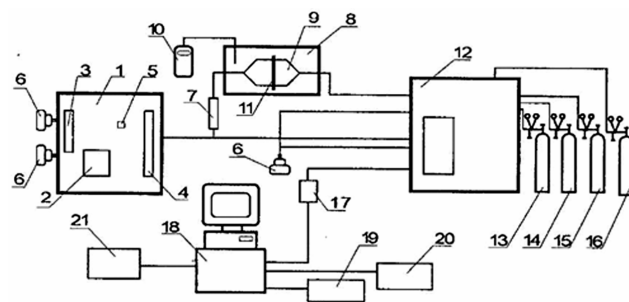
- continual generation of the benzene-air gas mixtures of stable concentrations and constant flow,
- calibration of GC/FID system by samples of benzene-air gas mixtures of differing concentrations and
- developing a calibration diagram of peak (chromatogram) *P<sub>s</sub>* surface dependence on benzene entry concentration in gas mixture *C<sub>0sd</sub>*, determined gravimetrically from daily change of mass of diffusion pipe and air flow [*P<sub>s</sub>* = *f*(*C<sub>0sd</sub>*)].

For the generation of benzene-air gas mixtures of required concentrations we used DYNA calibrator with diffusion pipe containing benzene. It was thermostated at required temperature. Rate of diffusion from the diffusion pipe was determined gravimetrically by an analytical scale with 0.1 mg accuracy. Benzene concentration in air mixture at the DYNA calibrator exit point is expressed by the following equation:

$$C = \frac{r}{Q_p + Q_d} = \frac{r}{Q_D} \quad \dots (1)$$

where *C* is the benzene concentration in air mixture (g/m<sup>3</sup>); *Q<sub>p</sub>*, the primary air flow above the diffusion pipe (m<sup>3</sup>/min); *Q<sub>d</sub>*, the additional air flow (m<sup>3</sup>/min); *Q<sub>D</sub>*, the total air flow at the exit point of DYNA calibrator (m<sup>3</sup>/min); and *r*, the rate of benzene diffusion from the diffusion pipe (g/min).

Because of the low diffusion rate and need of high temperatures for the experiments, we used a shortened



- |  |  |
|--|--|
| 1 — dyna Calibrator  | 12 — gas chromatograph   |
| 2 — chamber for thermostating diffusion pipe                           | 13 — FID air bottle  |
| 3 — flow controller for regulating the basic flow through the chamber  | 14 — FID hydrogen bottle   |
| 4 — flow controller for regulating the dilution flow                   | 15 — bottle with nitrogen as a carrier gas                                       |
| 5 — switch for regulating the flow of produced steam toward the filter | 16 — bottle with air for pneumatic pipe that injects gas mixture into the column |
| 6 — filters  | 17 — interface   |
| 7 — flow controller for regulating the steam flow to the sample        | 18 — computer  |
| 8 — chamber for thermostating of test cell                             | 19 — keyboard  |
| 9 — test cell  | 20 — printer   |
| 10 — digital temperature meter   | 21 — plotter   |
| 11 — sample  |  |

Fig. 2 — Schematic diagram of apparatus for determining benzene breakthrough curves

diffusion pipe known as DC<sub>Dskr</sub>. Ratio of cross-section and pipe height ( $A/L$ ) is found to be 0.089 cm. Mass of the diffusion pipe was determined daily, before and after the experiments. From the change in diffusion pipe mass  $\Delta m$  (mg) and benzene vapor emission time  $\Delta t$  (min), we calculated an average daily rate of diffusion by the equation  $r_{sd}(\text{mg}/\text{min}) = \Delta m / \Delta t$ .

Concentration of benzene in air gas mixture was kept changing only by changing the temperature in the DYNA calibrator chamber. Average daily benzene entry concentration [ $C_{0sd}$  ( $\text{g}/\text{dm}^3$ )] was determined from the average daily rate of diffusion ( $r_{sd}$ ) and the primary flow ( $Q_p$ ) through the chamber of the DYNA calibrator, using the relationship  $C_{0sd} = r_{sd} / Q_p$ . We used a peristaltic pump to direct a part of the prepared primary air flow with established benzene entry concentration towards the sample and the pneumatic loop of the GC/FID system, and the other part of air flow directly towards the pneumatic loop of the GC/FID system. Flow of the gas mixture through the sample was maintained at  $Q = 100 \text{ cm}^3/\text{min}$ , which corresponds to the linear velocity ( $u$ ) through the sample:  $u = Q / A_u = 10 \text{ cm}/\text{min}$ , where  $A_u$  is the marked sample cross-section ( $10 \text{ cm}^2$ ). For stable operation we used standard conditions such as nitrogen flow of  $50 \text{ cm}^3/\text{min}$ , hydrogen flow of  $50 \text{ cm}^3/\text{min}$ , air flow of  $330 \text{ cm}^3/\text{min}$ , injector temperature of 393 K, furnace temperature of 373 K and detector temperature of 443 K.

Time of sequence duration and number of sequences necessary for determining the curve of breakthrough were regulated by the appropriate computer program OBRADA:700,1<sup>13</sup> and have not been changed. Computer system attached to the GC/FID system was memorized to get prints of numerical values of benzene peak surface (chromatogram) which corresponds to ratio entry and exit concentrations, as well as retention time for the appropriate peak; ratio is expressed in per cent. Hence, there was no need to calibrate GC/FID system, especially in the area of low concentration breakthroughs.

### 2.3 Processing of Breakthrough Data

Benzene experimental breakthrough data ( $t, C_i/C_0$ ) from air current were processed by modified Yoon-Nelson model for an asymmetric S-curve, as shown below:

$$\ln \frac{P}{1-P} = -A + k'' \ln(W_a + t) \quad \dots (2)$$

where  $k''$  is the constant of the speed (YNM),  $\text{min}^{-1}$ ;  $A$ , the differential molar adsorption work,  $\text{kJ}/\text{mol}$ ; and

$W_a$ , the modified breakthrough time, as kinetic adsorption capacity depends on time (min).

The parameters  $k''$ ,  $A$  and  $W_a$  were determined by filtering experimental data ( $t, C_i/C_0$ ) using Gauss-Newton method of least squares for regression analysis of nonlinear function<sup>13</sup>. With the help of certain parameters you can calculate breakthrough times ( $t_{1\%}$  and  $t_{50\%}$ ), using the following equations:

$$\ln \frac{P}{1-P} = -A + k'' \ln(W_a + t_{p\%}) \quad \dots (3)$$

$$A = k'' \ln(W_a + t_{50\%}) \quad \dots (4)$$

Adsorbent layer breakthrough time ( $t_{1\%}$ ) represents a time interval (min), expires from the moment of gas mixture (benzene and air) directing the sample to the moment when benzene exit concentration achieves the value of  $C_i/C_0 = 0.01$  (it is 1 % breakthrough time,  $t_{p\%} = t_{1\%}$ ). When benzene exit concentration reaches the value of  $C_i/C_0 = 0.50$  ( $t_{p\%} = t_{50\%}$ ), a 50% breakthrough is achieved. Time of propagation ( $t_p$ ) was calculated using the program OBRADA:700,1, as an average time of retention of concentration ( $C_i = 0.999C_0$ ) in the adsorbent layer, using the following integral:

$$t_p = \int_0^{t_{99.9\%}} \left( 1 - \frac{C_i}{C_0} \right) dt \quad \dots (5)$$

Total saturation capacity ( $W_s$ ) of the adsorbent layer in the sample was not determined using software but was calculated using the following equation, from the 50 % breakthrough time, product flow  $Q$ , and the entry concentration  $C_0$ :

$$W_s = C_0 \cdot Q_{t_{50\%}} \quad \dots (6)$$

## 3 Results and Discussion

### 3.1 Dependence of Benzene Diffusion Rate on Temperature and FID Calibration

Table 1 shows the rate of diffusion ( $r_{sd}$ ) in  $\text{mg}/\text{mm}$ , average daily benzene entry concentrations ( $C_{0sd}$ ), and corresponding peak surfaces  $P_{s60}$  (average value of the chromatogram peak surface in the 60 min time interval) and  $P_{sd}$  (average daily value of the chromatogram peak surface) parameters, dependant on the diffusion pipe temperature ( $T$ ).

By correlating the experimental data with this exponential curve, we observe a dependence function related to the rate of diffusion, as shown below:

$$r_{sd} = 5 \times 10^{-9} e^{0.0595 \times T} \quad \dots (7)$$

$$R^2 = 0.996 \quad \dots (8)$$

On the basis of dependence Eqs (7) and (8) and the needed rate of diffusion  $r$  for the chosen benzene entry concentration and the primary flow through the DYNA calibrator chamber, we determined the necessary DYNA calibrator chamber temperature (338 K) for achieving the target benzene concentration, as given below:

$$r = C_0 \cdot Q_p = 2.80 \text{ mg/min} \quad \dots (9)$$

Based on the preliminary data (Table 1), we determined the functional dependence of peak surface and benzene entry concentration (Fig. 3.).

By correlating the experimental data with this exponential curve, we observed the dependence of  $P_{s60}$  on  $C_{0sd}$ , as given below:

$$P_{s60} = 83590e^{(0.0595 \times C_{0sd})} \quad \dots (10)$$

$$R^2 = 0.872 \quad \dots (11)$$

Benzene entry concentration ( $C_0$ ) 10  $\text{g/m}^3$  corresponds to  $P_{s60}$  value of 392.652 units of surface.  $P_{s60}$  and  $C_{0sd}$  values are given in Table 1.

Table 1 — Dependence of benzene diffusion rate ( $r_{sd}$ ) and concentration of benzene in air gas mixture on temperature of diffusion pipe and results of FID calibration

Temperature K	$r_{sd}$ mg/min	$C_{0sd}$ $\text{g/m}^3$	$P_{s60}$ ( $\sigma$ , $\sigma\%$ )	$P_{sd}$ ( $\sigma$ , $\sigma\%$ )
343	4.29	15.0	982 739 (25 684; 2.6 %)	1 012 699 (30 347; 3.0 %)
303	0.46	1.6	72 776 (3 506; 4.8 %)	-
313	0.55	1.9	108 928 (4 320; 2.6 %)	-
323	0.94	3.3	200 270 (9 324; 4.7 %)	-
333	1.92	6.7	403 572 (36 698; 9.0 %)	-
343	4.53	15.9	947 372 (70 036; 9.0 %)	-
338	2.83	9.9	281 345 (1 897; 0.7 %)	-
338	2.69	9.4	270 590 (2 394; 0.9 %)	269 452 (1947; 0.7 %)

Average value of primary air flow through DYNA calibrator chamber  $Q_p = 280 \text{ cm}^3/\text{min}$ , temperature of the surroundings  $296 \pm 1 \text{ K}$ .

**3.2 Determining Breakthrough Curves and Benzene Breakthrough Times**

Table 2 shows the dependence of benzene breakthrough experimental data ( $t, C_i/C_0$ ) on the sandwich material as well as parameters  $A$ ,  $k''$  and  $W_a$ . Table 2 also shows the dynamic adsorption properties of the sandwich material, such as  $t_{1\%}$ ,  $t_{1\%(10)}$ ,  $t_{p50\%}$ ,  $W_s$  and  $t_P$ .

One per cent breakthrough time  $t_{1\%(10)}$  represents an adjusted 1% time ( $t_{1\%,}$ ) determined for every sample with nominal concentration (10  $\text{g/m}^3$ ), according to the average daily concentration  $C_{0sd}$  ( $\text{g/m}^3$ ), using the following equation:

$$t_{1\%}(10) = \frac{C_{0sd} \cdot t_{1\%}}{10} \quad \dots (12)$$

Benzene breakthrough curve of sandwich materials (M1-2, M2-3, M2PUR-2 and M00-3) are shown in Fig. 4. Table 2 shows the comparison of experimental data for benzene breakthrough curves ( $t, C_i/C_0$ ) for CPO sandwich materials with assymetrical S-curves according to MYNM.

From Fig. 4 we observed that the 50 % benzene breakthrough for CPO-M1 sandwich material occurs in 7 min, while for CPO-M2PUP, it occurs in 70 min, for CPO-M2 in 138 min, and for CPO-M00 in 276 min. Hence, it is concluded that CPO-M00 has shown the best properties, followed by the CPO-M2, CPO-M2PUP and CPO-M1. Table 3 shows the  $k''$ ,  $A$  and  $W_a$  parameters of asymmetric S-curves according to the MYNM for sorption layers of examined CPO sandwich materials (TSUM M1, TSUM M2, TSUM M2PUP and TSUM M00), and determined by fitting experimental benzene breakthrough data ( $t, C_i/C_0$ ) with computed program.

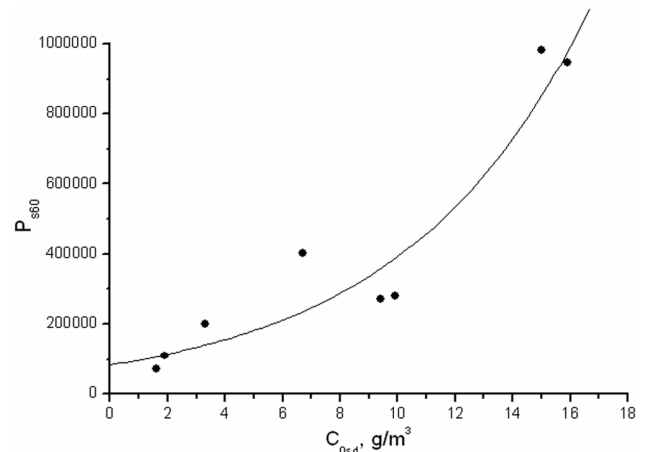


Fig. 3 — Dependence of peak surface ( $P_{s60}$ ) on average daily benzene entry concentration ( $C_{0sd}$ )

Table 2 — Comparison of experimental data of benzene breakthrough curves ( $t$ ,  $C_i/C_0$ ) on CPO sandwich materials with asymmetric S-curves according to MYNMM

Sample	Mass of sample and of adsorbed benzene from the change of sample mass, g		Sample thickness, mm	$r_{sd}$ mg/min	$C_{0ad}$ g/m <sup>3</sup>	$P_{su}$ ( $\sigma$ , $\sigma^0\%$ )	$A$	$k''$	$W_a$	$r$	$t_{1\%}$ min	$t_{1\%}$ (10) min	$t_{50\%}$ min	$W_s$ mg	$t_p$ min
	$m_u$	$m_s$ ( $\sigma$ , $\sigma^0\%$ )													
M1-1	0.9816			2.74	9.80	299 707 (5574; 1.9%)	5.514	1.414	0.198	0.996	1.7	1.7	49	48	122
M1-2	0.5814	0.690 (0.198; 29%)	0.012 (0.012; 96%)	2.74	9.79	206 821 (1 592; 0.8%)	2.935	-1.304	2.792	1.000	-2.5	-2.4	7	7	25
M1-3	0.5693			2.74	9.79	205 451 (475; 0.2%)	2.678	1.120	3.353	1.000	-3.2	-3.1	8	8	46
M2-1	0.7497			2.83	10.10	226 904 (16 308; 7.2%)	14.241	2.895	1.780	0.997	26.2	26.5	35	35	166
M2-2	0.6690	0.719 (0.043; 6%)	0.040 (0.002; 6%)	2.84	10.15	200 971 (4 927; 2.4%)	21.556	4.142	26.760	1.000	33.3	33.8	55	56	174
M2-3	0.7373			2.77	9.91	205 906 (3 182; 1.5%)	22.185	4.337	28.378	1.000	29.3	29.0	138	137	153
M2PUP-1	0.7630			2.76	9.84	217 861 (4 529; 2.1%)	9.977	2.414	7.200	0.996	2.1	2.1	55	54	76
M2PUP-2	0.7569	0.783 (0.039; 1%)	0.024 (0.003; 14%)	2.74	9.79	199 806 (3 058; 1.5%)	9.577	2.206	6.696	0.997	2.9	2.8	70	69	102
M2PUP-3	0.8280			2.74	9.79	206 717 (605; 0.3%)	12.252	2.735	16.341	0.999	0.1	0.1	72	70	94
M00-1	1.0367			2.29	9.80	216 931 (2 416; 1.1%)	10.785	1.945	-57.566	0.989	81.7	80.1	313	307	462
M00-2	0.9790	0.996 (0.035; 4%)	0.072 (0.004; 6%)	2.76	9.86	216 212 (2 068; 1.0%)	14.478	2.690	-23.650	0.992	63.1	62.2	241	238	298
M00-3	0.9726			2.69	9.62	203 879 (3 681; 1.8%)	23.888	4.142	43.356	0.999	62.1	59.7	276	266	309

Benzene entry concentration ( $10 \pm 1$ ) g/m<sup>3</sup>, experimental temperature ( $296 \pm 1$ ) K, saturation concentration of benzene ( $C_s$ ) 367 g/m<sup>3</sup>, which corresponds to a relative pressure of ( $p_r$ )  $\approx 0.03$ . Flow through sample(Q) 0.1 dm<sup>3</sup>/min.



Also shown are some dynamic adsorption properties of examined TSUM samples, such as  $t_{1\%}$ ,  $t_{1\%(10)}$ ,  $t_{p50\%}$ ,  $W_s$  and  $t_p$ .

Comparison of benzene breakthrough curves CPO materials (M1-2, M2-3, M2PUP-2 and M00-3) with appropriate breakthrough curves on sorption layers is shown in Fig. 5.

Table 4 shows the benzene breakthrough experimental data with computer software as well as parameters  $k''$ ,  $A$  and  $W_a$  of asymmetric S-curves according to MYNM for TSUM samples. Also the results of determining the 1 % breakthrough time  $t_{1\%}$  and  $t_{1\%(10)}$  are shown.

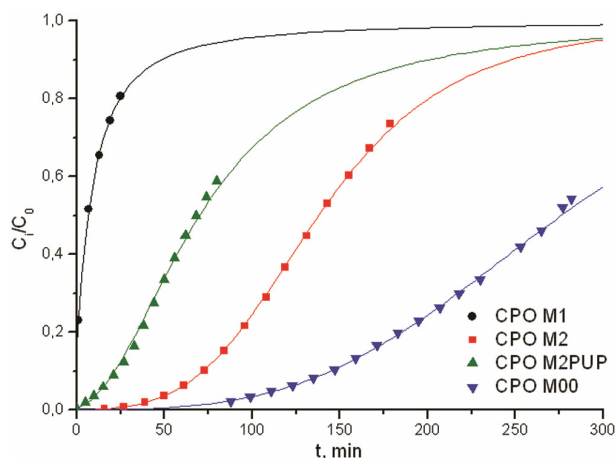


Fig. 4 — Comparison of benzene breakthrough curves of selected characteristics of CPO sandwich materials

Comparison of benzene breakthrough curves of CPO inner layer (M1, M2, M2PUP and M00) with breakthrough curves on TSUM of foreign manufacturers (HLS<sub>pur</sub> 2084) on the basis of both polyurethane foam and filter cloth type Saratoga (SFG<sub>stg</sub> 3002 and BCH<sub>stg</sub>) is shown in Fig. 6.

For comparing the current results with the results obtained using benzene with similar materials, we

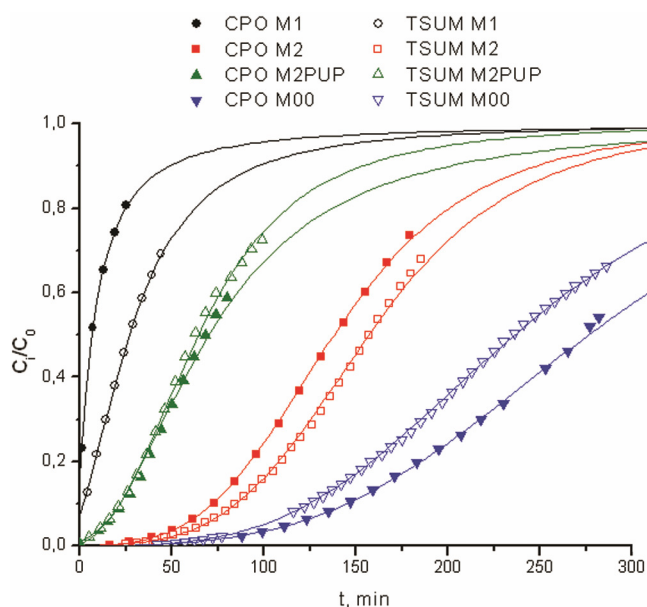


Fig. 5 — Comparison of benzene breakthrough curves of different samples of CPO sandwich materials

Table 3 — Comparison of experimental data of benzene breakthrough curves ( $t$ ,  $C_t/C_0$ ) on sorption layers of CPO sandwich materials with asymmetric S-curves according to MYNM

Characteristic	TSUM M1	TSUM M2	TSUM M2PUR	TSUM M00
Sample mass, g	0.5948	0.4980	0.4622	0.6523
Mass of adsorbed benzene, g	0.0142	0.0446	0.0265	0.0596
Sample thickness, mm	1.02	0.80	0.13	0.83
$r_{sd}$ , mg/min	2.77	2.73	2.74	2.72
$C_{osd}$ , g/m <sup>3</sup>	9.91	9.74	9.78	9.73
$P_{sy}$ ( $\sigma$ , $\sigma\%$ )	202 122 (11 878; 5.9 %)	202 640 (6 256; 3.1 %)	208 666 (3594; 1.7 %)	209 381 (1971; 0.9 %)
$A$	7.728	26.412	13.167	20.866
$k''$	2.117	4.975	2.987	3.771
$W_a$	11.635	45.100	17.814	17.058
$r$	1.000	1.000	0.999	1.000
$t_{1\%}$ , min	-7.2	35.1	-0.2	57.8
$t_{1\% (10)}$ min	-7.1	34.2	-0.2	77.9
$t_{50\%}$ , min	27	157	64	236
$W_s$ , mg	27	153	63	223
$t_p$ , min	45	171	81	267

Initial benzene entry concentration ( $C_0$ ) =  $(10 \pm 1)$  g/m<sup>3</sup>, temperature was  $(293 \pm 1)$  K, benzene saturation concentration ( $C_s$ ) = 322 g/m<sup>3</sup>, and relative benzene pressure ( $p_r$ )  $\approx$  0.03. Benzene-air gas mixture flow through the sample ( $Q$ ) = 0.1 dm<sup>3</sup>/min.

Table 4 — Comparison of experimental benzene breakthrough curve data ( $t, C_i/C_0$ ) on TSUM of foreign manufacturers calculated with assymetric S-curves according to MYNM

Adsorbent label	$C_{0sd}$ $g/m^3$	$A$	$k''$	$W_a$	$r$	$t_{1\%}$ min	$t_{1\%}(10)$ min
HSF <sub>pur</sub> 2084	10.4	18.953	4.230	2.513	1.000	9.3	9.7
SFG <sub>stg</sub> 3002	10.4	48.998	9.319	88.140	0.999	27.8	28.9
BCH <sub>stg</sub>	9.3	38.841	8.213	39.586	0.999	25.1	23.4

Initial benzene entry concentration ( $C_0$ ) ( $10 \pm 1$ )  $g/m^3$ , experimental temperature ( $293 \pm 1$ ) K. Benzene-air gas mixture flow through the sample ( $Q$ )  $0.1 dm^3/min$ .

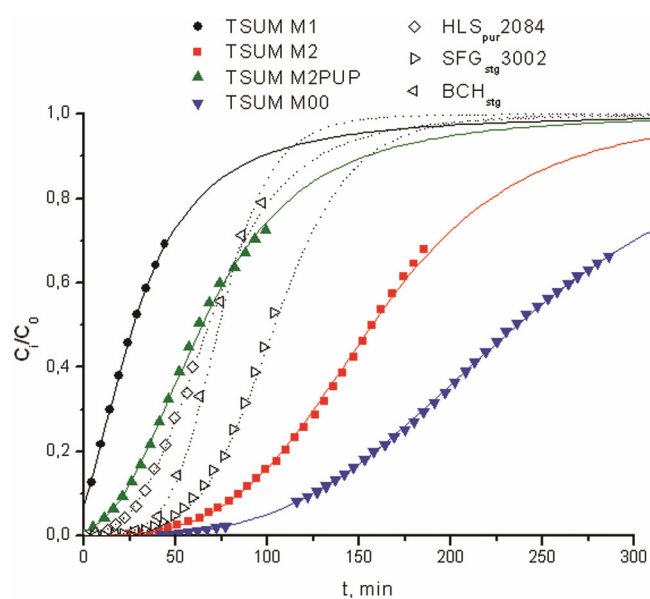


Fig. 6 — Comparison of benzene breakthrough curves of different samples of sorption layers

chose a previously used benzene concentration in the air gas mixture ( $C_0 = 10 g/m^3 = 0.13 mmol/g$ ;  $p_r = p/p_0 = C_0/C_s \approx 0.03$ ). The results show that the CPO - M00 has the best quality properties.

It is thus pointed out that the results obtained have created conditions for the development of a functional model which can be used as an efficient means for body protection in the future, according to the new technological development<sup>14,15</sup>.

#### 4 Conclusion

- 4.1 It is found that TSUM CPO-M00 sandwich material has much better protective properties when compared with other thin layered sorption carbon materials used for protective gear.
- 4.2 A benzene entry concentration in an air gas mixture of  $10 mg/dm^3$  has been chosen and successfully achieved this concentration by using diffusion pipe  $DC_{Dskr}$  ( $A/L = 0,089 cm$ ) that was thermostated in a DYNA calibrator chamber at 338 K. The rate of

benzene diffusion from the pipe which matches this concentration is  $2.80 mg/min$  and the average chromatogram surface of the examined samples is  $P_{sus}$  od 281345 units ( $\sigma = 11 \%$ ).

- 4.3 Benzene breakthrough curves in chosen conditions has been obtained for four types of CPO sandwich materials (each with three samples) at one sample of sorption layers of these materials, without the masking layer.
- 4.4 Experimental data of benzene breakthrough curves on examined samples ( $t, C_i/C_0$ ) has been analyzed by fitting using the computer program OBRADA:700,1, with assymetric S-curves according to MYNM. We determined basic system dynamic parameters, such as  $k''$ ,  $A$  and  $W_a$ ,  $t_{1\%}$ ,  $t_{1\%}(10)$ ,  $t_{50\%}$ ,  $W_s$  and  $t_p$  and compared them to each other.
- 4.5 CPO-M00 sandwich material has an obvious advantage over other types of CPO sandwich materials in dynamic conditions.
- 4.6 The benzene breakthrough curves in chosen conditions have also been developed on sorption layers of CPO sandwich materials and determined system dynamic parameters by fitting experimental data ( $t, C_i/C_0$ ) through computer program using assymetric S-curves according to MYNM. Obtained breakthrough curves and dynamic system parameters are compared with appropriate results obtained for CPO sandwich materials.
- 4.7 Comparison of benzene breakthrough curves on delivered CPO sandwich materials with breakthrough curves on sorption layers of these materials does not give a generally visible trend of differences which we could consider to be within the interval of experimental error. Breakthrough curves on sorption layers have somewhat larger correlation coefficients with points that we obtained experimentally.
- 4.8 CPO type TSUM sandwich material sorption layer has an obvious advantage over the two



examined types of foreign thin layered sorption materials on the basis of Saratoga™ filter cloth when looking at the effects of benzene in dynamic conditions.

According to the modern tendencies of development and implementation of new technologies, these results can promote the development of the contemporary personal protective equipment.

### Acknowledgement

Authors acknowledge with thanks the funding support by the Ministry of Education, Science and Technological Development of the Republic of Serbia [Grant No. TR34034 (2011-2014)].

### References

- 1 Karkalic R, *Optimization of thin layered active charcoal sorption materials embedded into the NBC protective materials in the function of protective characteristics and physiologic compliance*, Ph.D. thesis, Military Academy, Belgrade, 2006.
- 2 Wilusz E, *Polymeric Materials Encyclopedia* (CRC Press, Boca Raton), 1996.
- 3 Nieminen M, Ranta J, Laine J & Nousiainen P, *Stud Surf Sci Catal*, 87 (1994) 689.
- 4 Rivin D & Kendrick C, *Carbon*, 35 (1997) 1295.
- 5 Truong Q & Rivin D, *Testing and Evaluation of Waterproof/Breathable Materials for Military Clothing Applications*, NATICK/TR-96/023L (US Army Natick RD&E Center, Natick), 1996.
- 6 Lee T, Ooi C H, Othman R & Yeoh F Y, *Rev Adv Mater Sci*, 36 (2014) 118.
- 7 Barton S S, Boulton G L & Harrison B H, *Carbon*, 10 (1972) 395.
- 8 Truong Q & Wilusz E, in *Smart Textiles for Protection*, edited by R A Chapman (Woodhead Publishing Limited, New Delhi, India), 2013.
- 9 Nurfaizey A H, Tucker N, Stanger J & Staiger M P, in *Functional Nanofibers and their Applications*, edited by Q Wei (Woodhead Publishing Limited, New Delhi, India) 2012.
- 10 Bastić J, *Dynamic method for testing of protective sorption materials*, Ph.D. thesis, Faculty for Technology and Metallurgy, Belgrade, 1995.
- 11 Yoon Y H & Nelson J H, *Am Ind Hyg Assoc J*, 45 (1984) 509.
- 12 Petrović V & Bočvarov N, Program OBRADA:7000,1 for experimental procedure, V102, program language BASIC 5.1 for HP-300 Serie 9000 (Military Technical Institute, Belgrade), 1994.
- 13 Ivanović S, *The influence of porous structure of granulated charcoal to benzene absorption speed*, M.Sc thesis, Faculty of Physical Chemistry, Belgrade, 1996.
- 14 Cukierman A L, *ISRN Chem Eng*, 2013 (2013) 1.
- 15 Ching-Iuan S, Te-Li S & Yi-Ching C, *Polym-Plast Technol*, 53 (2014) 1012.